Effects of Hard-Segment Compositions on Properties of Polyurethane–Nitrolignin Films

LINA ZHANG, JIN HUANG

Department of Chemistry, Wuhan University, Wuhan 430072, People's Republic of China

Received 27 July 2000; accepted 7 November 2000

ABSTRACT: Segmented polyurethane (PU) films from castor-oil-based PU prepolymer with different hard-segment compositions and nitrolignin (NL) were synthesized. Diisocyanates (DIs), such as 2,4-tolylene DI (TDI) and 4,4′-diphenylmethane DI (MDI), 1,4-butanediol (BDO) as a chain extender, and trimethanol propane (TMP) as a crosslinker were used to obtain PU films containing NL (UL) which were named as UL–TB for TDI and BDO, UL–TT for TDI and TMP, UL–MB for MDI and BDO, and UL–MT for MDI and TMP, respectively. The mechanical properties and thermal stability of the films were characterized by a tensile test and thermogravimetric analysis, respectively. The MDI-based UL films exhibited a higher tensile strength (σ_b) and thermal stability than TDI-based UL. However, the recoverability of the TDI-based UL films was better than that of others. The UL films with TMP (UL–TT and UL–MT) had higher σ_b and lower breaking elongation (ϵ_b) than the UL films with BDO (UL–TB and UL–MB), caused by enhancement in the crosslinking network of hard segments and microphase separation between soft and hard segments. The values of σ_b and ϵ_b of the UL films that contained NL were much higher than those of the PU films, which indicates that the introduction of NL increased the interaction between hard segments by crosslinking. The hydrogen bonding in the UL films was studied by infrared spectroscopy, which indicated that MDI favored the formation of hydrogen bonds, especially in the ordered domain. Differential scanning calorimetry, dynamic mechanical analysis, and wide-angle X-ray diffraction indicated that the UL films were compatible as a whole, but microphase separation existed between soft and hard segments and significantly affected the mechanical properties. © 2001 John Wiley & Sons, Inc. J Appl Polym Sci 81: 3251–3259, 2001

Keywords: nitrolignin; polyurethane; hard-segment compositions; mechanical properties; hydrogen bonding; microphase separation

INTRODUCTION

It is well known that polyurethane (PU), a segmented block copolymer, constitutes a class of very useful and versatile materials that consist of alternating soft and hard segments. The versatile and interesting properties of segmented PU are generally attributed to the formation of a microphase-separated structure that arises from the thermodynamic incompatibility of the glassy hard-segment and rubbery soft-segment sequences.[1] Soft segments are usually composed of moderate molecular weight (600–4000) polyether- or polyester-polyols, and hard segments are obviously formed in a polyaddition reaction of diisocyanate (DI) with low molecular weight (60–400) difunctional or multifunctional alcohols or amines that act as chain extend-

Correspondence to: L. Zhang (lnzhang@public.wh.hb.cn).

Contract grant sponsor: National Natural Science Foundation of China; contract grant number: 59773026.

Contract grant sponsor: National Natural Science Foundation of China; contract grant number: 59933070.

Contract grant sponsors: Laboratory of Molecular Engineering of Polymers, Fudan University; Laboratory of Cellulose and Lignocellulosic Chemistry, Guangzhou Institute of Chemistry, Chinese Academy of Sciences.

Journal of Applied Polymer Science, Vol. 81, 3251–3259 (2001)

ers or crosslinkers.[2] Phase separation is of primary importance because it strongly affects the properties and gives rise to the interesting and useful properties of PU materials.[3] A basic understanding of the effects of this structure on the properties of PUs is essential for the practical application in a broad range. The microphase separation between hard-segment domains and the soft-segment matrix has mainly been demonstrated by infrared (IR) spectroscopy,[1–7] differential scanning calorimetry (DSC),[1,8–13] dynamic mechanical analysis (DMA),[8,11,13] and wide-angle X-ray diffraction (WXRD).[10,11,14]

The unique elastomeric properties of PU are caused by microdomain formation, and hard-segment domains provide both physical crosslinking sites and filler-like reinforcement to the soft-segment matrix.[10] The introduction of a triol functional group into the hard segments increases the aggregation of the hard segments through crosslinking covalent bonds, which results in the microphase separation of the soft and hard segments.[9] However, the presence of a triol crosslinker in the hard segments results in a decrease in the aggregation of hard segments through hydrogen bonding, caused by the highly steric hindrance, and the degree of microphase separation of soft and hard segments decreases with the increase in triol crosslinker content.[1] Therefore, the structure and morphology of the segmented PUs are very complex. The different DIs also affect the structure and properties of segmented PU. Seefried et al.[15] showed that 4,4′-diphenylmethane diisocyanate (MDI)-based PU, in contrast to 2,4-tolylene diisocyanate (TDI)-based PU, possesses a more perfect domain organization because of a short-range order, including crystallinity. MDI-based PU exhibited higher tensile properties, lower elongation, and higher thermal stability than TDI-based PU in a 1,4-butanediol (BDO)/polyester/DI system.[16] Moreover, a hydroxyl-terminated polybutadiene/trimethanol propane (TMP)/TDI system with microphase separation showed the highest tensile strength (σ_b), whereas a polypropylene glycol/TMP/MDI system exhibited the highest breaking elongation (ϵ_b).[17]

In previous work,[18] PU–nitrolignin (PUNL) films were satisfactorily synthesized from castor-oil-based PU prepolymer and nitrolignin (NL) that had a weight-average molecular weight (M_w) of 20.6×10^4 and a highly branched structure. The σ_b and ϵ_b of PUNL films with 2.8% NL were two times higher than those of PU films. NL in hard segments played an important role in the enhancement of the mechanical properties of PUNL. In this study, we attempted to explore the effects of the hard segments on polyurethane containing NL (UL). The different DIs (MDI and TDI), BDO as a chain extender, and TMP as a crosslinker were arranged in four groups to prepare UL films with different hard-segment compositions. The mechanical and thermal properties of the UL films were evaluated by a tensile test, thermogravimetric analysis (TGA), DSC, and DMA. The interaction of hydrogen bonding and the morphology in the UL films were investigated by IR, WXRD, and the previously mentioned methods and are discussed.

EXPERIMENTAL

Materials

All the chemical reagents were obtained from commercial resources in China. Alkali lignin from bamboo was supplied by Guangzhou Chemistry Institute (Guangzhou, China). Chemically pure castor oil was dehydrated at 100°C under 20 mmHg for 1 h. TDI was redistilled before use, and MDI was obtained from Bayer Co. (Germany). BDO from Medicine Group of China and TMP from First Chemical Reagent Factory of Shanghai were used as a chain extender and a crosslinker, respectively.

Synthesis of NL and PU

The NL was prepared and characterized according to a former method.[18] The measurement of the N content in NL was performed on a Heraeus elemental analyzer (CHN-O-RAPID, Germany). M_w's of NL were determined with a multiangle laser photometer equipped with a He–Ne laser of $\lambda = 633$ nm (DAWN-DSP, Wyatt Technology Co., Santa Barbara, CA) in tetrahydrofuran (THF) at 25°C and at 18 angles. The NL solutions with concentration of $0.88–4.45 \times 10^{-3}$ g/mL) were filtered with a series of filters (0.45 and 0.20 μm; Whatman, England) directly into a scintillation vial. The specific refractive-index increment (dn/dc) was obtained on a double-beam differential refractometer (DRM-1020, Otsuka Electronics Co., Japan) at 633 nm and 25°C to be 0.149 mL/g for NL in THF. Astra software was used for data acquisition and analysis. The characteristics of two NLs named NL I and NL II were determined to have a N content 8.08 and 6.32% and M_w's of 19.2×10^4 and 20.6×10^4, respectively.

Table I Overall Composition of All Samples

Sample	Isocyanate	Alcohol[a] (AO)	Weight Ratio of PUP/AO/NL[b]
UL–TB[c]	TDI	BDO	3.0/0.45/0.10
UL–TB-II[c]	TDI	BDO	3.0/0.45/0.10
UL–TT	TDI	TMP	3.0/0.45/0.10
UL–MB	MDI	BDO	3.3/0.45/0.11
UL–MT	MDI	TMP	3.3/0.45/0.11
PU–TB	TDI	BDO	3.0/0.45/0
PU–TT	TDI	TMP	3.0/0.45/0
PU–MB	MDI	BDO	3.3/0.45/0
PU–MT	MDI	TMP	3.3/0.45/0

[a] BDO as a chain extender and TMP as a crosslinker.
[b] The NCO/OH molar ratio of different PUP and AO was controlled to be equal, and the NL content in UL series was 2.8%.
[c] NL I and II were used to prepare the films corresponding UL–TB and UL–TB-II, respectively.

Castor oil was added slowly with stirring to a round-bottom flask with DI (TDI or MDI). The reaction was carried out at 45°C for 50 min to produce the PU prepolymer (PUP). The equivalent weight per —OH of castor oil was 345 g, and that of TDI and MDI per —NCO was 87 and 125 g, respectively. From these three values, the NCO/OH molar ratio of the PU prepolymer was calculated to be 2.0.

The compositions of the PU and UL films are listed in Table I. The PU films were prepared by casting on a glass plate from a mixture of the PU prepolymer/THF solution and the BDO/THF or TMP/THF solution and then cured at 35 ± 2°C for 4 h (PU with MDI) or 7 h (PU with TDI). After they were completely cured, the films were placed in boiling water, and removed from the glass plate to obtain colorless films 0.15 mm thick, coded PU–TB, PU–TT, PU–MB, and PU–MT. The UL films were prepared from a mixture of the PU prepolymer/THF, NL/THF, and BDO/THF or TMP/THF solutions, followed by casting on a glass plate. The reddish-brown films, which were about 0.15 mm thick and were coded UL–TB, UL–TB-II, UL–TT, UL–MB, and UL–MT, were obtained via the curing and removal process previously mentioned.

Characterization

IR Spectroscopy

Fourier transform infrared (FTIR) spectra of the UL films were taken with KBr plates on a FTIR spectrometer (Nicolet 170SX, USA) in a wave number range of 4000–400 cm^{-1}.

WXRD

WXRD patterns of the UL films were recorded on a D/max-1200 X-ray diffractometer (Rigaku, Japan) with Cu Kα radiation ($\lambda = 1.5405 \times 10^{-10}$ m), and the samples were examined with 2θ values ranging from 6 to 40° at a scanning rate of 10°/min.

Mechanical Properties

The mechanical properties [σ_b, ϵ_b, and Young's modulus (E)] of the PU and UL films were measured on a universal testing machine (CMT6503, Shenzhen SANS Test Machine Co. Ltd., Shenzhen, China) with a testing rate of 100 mm/min according to ISO6239-1986 (E).

Recoverability Test

The samples of the PU and UL films were all marked to be 50 mm in length (l_0) and then snapped on a universal testing machine, previously mentioned, with a tensile rate of 100 mm/min. The length (l_1) of broken sheets was determined repeatedly after 12-h intervals. The recoverability (Re) of dimension was represented by

$$Re = \frac{l_0 - \Delta l}{l_0} \times 100\%$$

where Δl is the length of irrecoverable creep after 12 h and is equal to $l_1 - l_0$.

Thermal Properties

TGA curves of the UL films were recorded on a TG 209 thermoanalyzer (Netzsch Co., Germany) under an air atmosphere from 20 to 800°C at a heating rate of 10°C/min.

DSC

DSC measurements of the UL films were carried out on a DSC-2C thermal analyzer (Perkin-Elmer Co., USA). The heating rate was 10°C/min in a temperature range of −50 to 240°C.

DMA

DMA of the UL films was performed on a DMA 242 (Netzsch Co.) at a frequency of 1 Hz with the temperature ranging from −100 to 150°C and at a heating rate of 10°C/min.

Table II Mechanical Properties of Segmented PUs With and Without NL

Sample	σ_b (MPa)	ε_b (%)	E (MPa)	Re (%)
UL–TB	3.0	496	0.9	99
UL–TB-II	2.7	479	0.7	98
UL–TT	17.5	207	24.1	100
UL–MB	10.9	326	1.6	93
UL–MT	18.8	249	12.8	94
PU–TB	1.5	266	1.2	100
PU–TT	13.1	129	49.0	100
PU–MB	5.3	297	2.4	97
PU–MT	14.0	157	22.8	99

RESULTS AND DISCUSSION

Mechanical Properties of the Films

The mechanical properties of the UL and PU films are listed in Table II. The σ_b and ϵ_b values of the UL films that contained NL were all much higher than those of PU. This is in good agreement with a previous conclusion[18] that indicated that NL promotes the formation of the crosslinking network in the hard-segment domain of UL films, which results in an increase of attractive forces between hard segments. The E's of the UL films were lower than those of PU with the same hard-segment compositions, which suggests that the UL films had relatively high flexibility. The MDI-based UL films exhibited higher values of σ_b than TDI-based UL films with the same polyols; this may be caused by the formation of a three-dimensional network.[18] Simultaneously, UL–MB showed a lower ϵ_b and a higher E than UL–TB, which is consistent with the previous report that the high functionality of MDI causes a high degree of crosslinking and, consequently, reduces the elongation and imparts a high modulus and hardness in a different DI/BDO system.[16] The UL films with TMP had higher σ_b and E values and lower ϵ_b values than BDO-based UL films with the same DI. This mainly resulted from TMP with multifunctional groups that were attributed to the formation of a three-dimensional network. Triol-based PU not only had the simple physical crosslinking of hydrogen bonds similar to diol-based PU but also resulted in the formation of chemical crosslinking. UL–MT films, which consisted of MDI-based PU prepolymer, NL, and TMP, had the highest σ_b, caused by the enhancement in the crosslinking network, and UL–TB exhibited the lowest E value, which corresponded to highest flexibility.

The UL–TB and UL–TB-II films (from NL I and NL II, respectively) exhibited lower σ_b and higher ϵ_b than those (σ_b = 22.9 MPa, ϵ_b = 258%) of PUNL2 that were prepared from the same content of NL II, TDI, and BDO in a previous work;[18] this mainly resulted from the reduction of curing time, the changes of curing mold, and the removal condition. The UL films based on two NLs with different N contents and M_w's showed a slight difference, which suggests that a relatively higher N content and lower M_w may benefit the mechanical properties.

Strain recoverabilities (Re) of the UL and PU films are summarized in Table II. Wholly PU films could be more fully and speedily resiled than UL films. Usually, the dimensional stability of PU was imparted by hard segments; thus, the MDI-based PU and UL films had a lower Re than TDI-based films because of the flexibility imparted by —CH_2— groups in MDI. The PU films exhibited better Re than the UL films, which suggests that the introduction of NL increased the interaction between hard segments by crosslinking and chain stiffness. In all, the introduction of NL increased the strength and toughness because of the high degree of crosslinking caused by many functional groups in the highly branched NL.[18]

Thermal Stability of the Films

The three distinct stages of decomposition for PUs, which correspond to a previous article,[18] also occurred in the TGA curves of the UL films, as shown in Figure 1. The shapes of TGA curves for the MDI-based UL films were similar, and so were those of TDI-based UL films. Detailed data are listed in Table III, which shows that the MDI-based UL films exhibited a higher thermal stability than TDI-based UL films. Simultaneously, the decomposition behaviors of the UL films with TMP were similar to the behaviors of UL with BDO for two kinds of DI, which suggests that in this system, the increase in the crosslinking degree in the hard-segment domain hardly influenced the thermal stability. The higher decomposition temperature of the MDI-based UL films, such as UL–MB and UL–MT, at the same weight loss as TDI-based UL films was mainly caused by the stronger interaction between MDI and polyols.

Structure and Morphology of the Films

IR spectra of —C═O in the UL films are shown in Figure 2. —NH of PU could be hydrogen-bonded

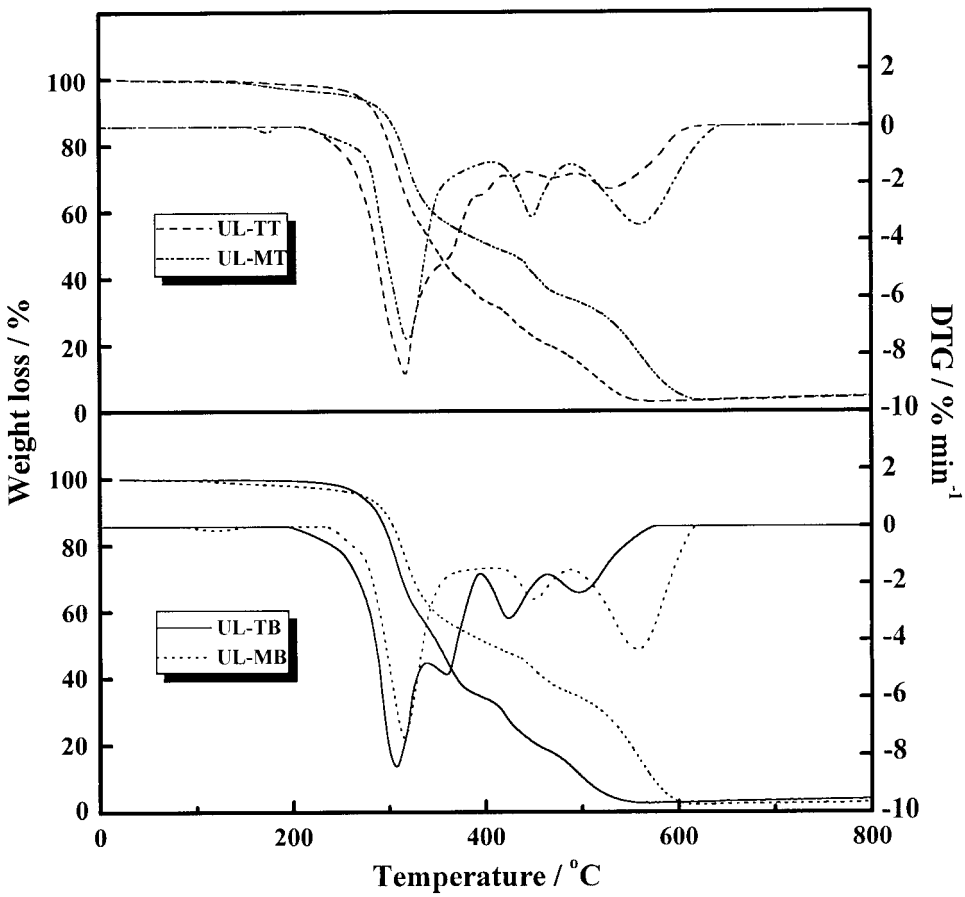

Figure 1 TGA curves as a function of temperature for UL films.

with the urethane —C═O of the hard segments and the ether- or ester-oxygens of the soft segments, and the hydrogen-bonded —C═O represents the extent of the hard–hard-segment bonding and hard–soft-segment bonding, respectively. The band in the —C═O stretching vibration amide-I region consists of three distinct bands due to hydrogen-bonded —C═O in ordered crystalline domains (1697–1706 cm^{-1}) and disordered amorphous domains (1714–1718 cm^{-1}) and free —C═O (1731–1734 cm^{-1}).[1] The band of —C═O for the UL films consists of three peaks located at 1734, 1714, and 1702 cm^{-1}. It was obvious that the absorbance of free —C═O in MDI-based UL films was much weaker than that in TDI-based UL films, which suggests that MDI favored the formation of hydrogen bonds. The peak intensities at 1702 cm^{-1} for the MDI-based UL films were stronger than those for TDI-based UL films, and the comparison of the peak intensities at 1714 cm^{-1} was adverse, which suggests that different DIs affected the distribution of hydrogen-bonded —C═O in the ordered and amorphous domains of the films. The absorbance at 1702 cm^{-1} for the UL–MT films was stronger than that of others, which suggests that strong intermolecular hydrogen bonding existed between the soft and hard segments in the UL–MT films and led to the reduction of microphase separation. In addi-

Table III Decomposition Temperature of the UL Films

Degradation (%)	Temperature (°C)			
	UL–TB	UL–TT	UL–MB	UL–MT
10	287	286	295	291
25	307	307	317	319
40	328	325	346	345
50	350	346	404	403
60	369	371	460	454
80	452	465	550	552
90	501	516	573	580

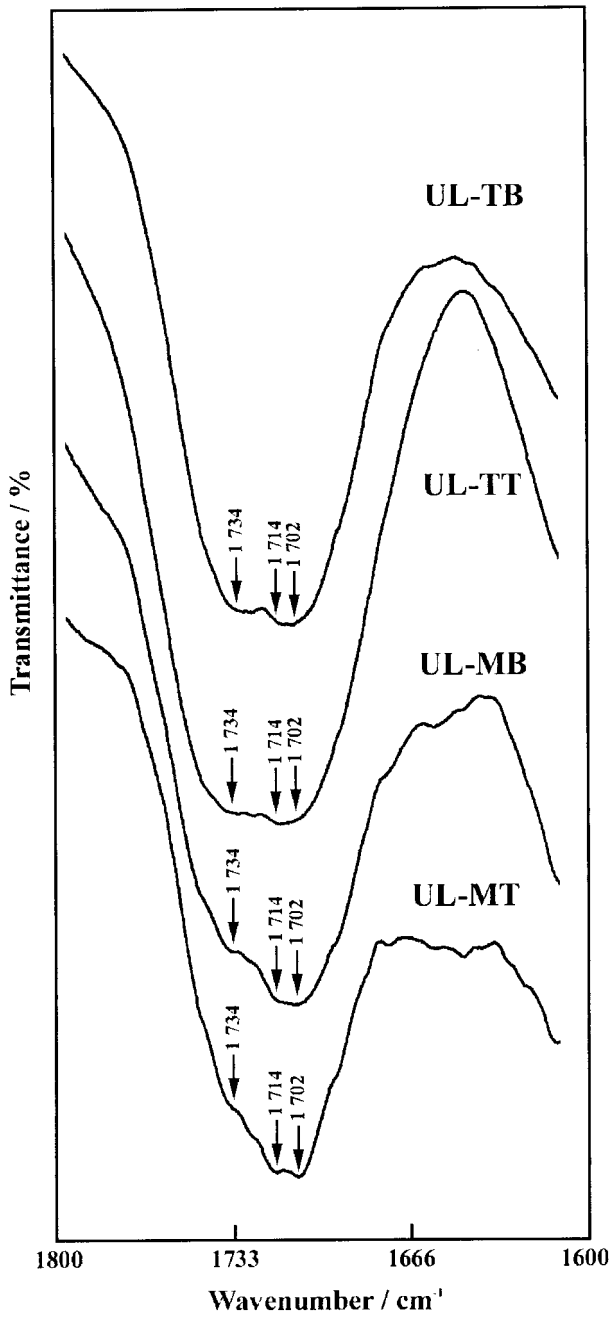

Figure 2 IR spectra of —C═O for the UL films.

tion, the second composites (BDO as extenders and TMP as crosslinkers) hardly influenced the absorbance of —C═O in UL films, which was depicted by the similar shape and intensity of free —C═O peaks. However, TMP affected the distribution of hydrogen bonds in the ordered and amorphous region and, hence, caused a peak at 1714 cm^{-1}, which was stronger because of the steric hindrance and asymmetry of TMP.

WXRD patterns of the UL films are shown in Figure 3, and the position of peaks, corresponding *d*-spacing values, and crystallinity degrees for every sample are listed in Table IV. The crystallinity degrees lie in a range of 0.40–0.42, showing mainly amorphous state. The small difference between the UL films suggested more ordering regions in the MDI-based UL films. Combined with the results of DSC, the broad peak III located at about 20° represents the existence of short-range ordering in the hard-segment domains.[8] The positions of peak III for the UL films shifted slightly to lower angles with the increase in the glass-transition temperature (T_g) for corresponding films, which was most likely caused by an increase in the hard-segment domain order. In addition, peaks I and II, located at about 7.7 and 9.4°, respectively, proved the existence of long-range ordering, which was not shown by DSC.

DSC curves of the UL films are shown in Figure 4, and the glass transition and other thermal transitions are detailed by the data in Table V. The UL–MT films had a higher T_g, caused by TMP with three functional groups, which led to a higher aggregation of hard segments by crosslinking with covalent bonds, which hindered the hydrogen-bond formation in the hard segments caused by the highly steric hindrance. The UL–TB films exhibited a lower T_g than others. As shown in Figure 4, the UL films all had dominant melting endotherms (T_{m2}'s) of short-range ordering in the hard segments, which corresponded to the domain size of the hard-segment ordering. The UL films with TMP exhibited the higher T_{m2} than UL with BDO, which indicated that TMP with three functional groups increased the size of the ordered hard-segment domains. T_{m2} values of the TDI-based UL films were slightly higher than that of MDI-based UL films with the same polyols, which suggests that the asymmetry of TDI increased the size of the ordered hard-segment domains. The melting enthalpy (ΔH_{m2}) was proportional to the intensity of the hard-segment hydrogen bonding and, thus, proportional to both the size and number of ordered hard-segment domains.[1] The UL–MT film exhibited higher ΔH_{m2} than UL–TT. Therefore, MDI increased the number of ordered hard-segment domains because of the formation of hydrogen bonding. This was supported by the results from IR spectroscopy.

The storage modulus (log E') and tan δ as a function of temperature from DMA for the UL films are shown in Figure 5. The DMA technique generally provides higher T_g values than DSC

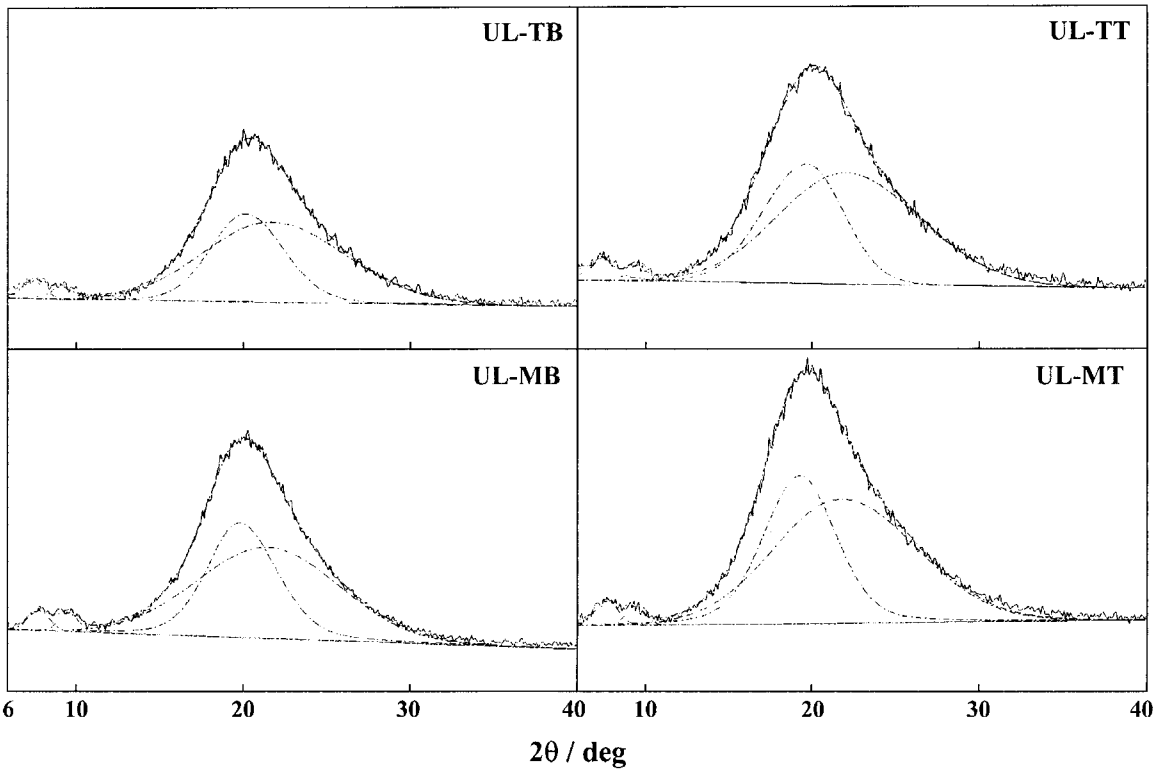

Figure 3 WXRD patterns as a function of 2θ for the UL films.

(usually up to 10°C higher) because of the dynamic nature of the test.[19] The intensities and positions of tan δ peaks were in the following order: UL–TT > UL–MT > UL–MB > UL–TB. The molecules in the UL–TB film were more easily removed than others. The sharpness and height of loss peaks gave information about the compatibility, degree of order, and molecular motion in the soft-segment matrix, whereas the position of the loss peak (T_{max}) provided details about the degree of microphase separation. All the UL films displayed one prominent loss peak, suggesting that they all were wholly compatible. The UL films with relatively great heights of the loss peak exhibited more amorphous region. The UL–TB film with TDI and BDO had better flexibility at lower temperatures than others because of the microphase separation between the soft and hard segments, which resulted in the freedom of molecular motion.

Table IV Detailed Data of WXRD Measurement for the UL Films

Sample	2θ (°)/d (Å)			Crystallinity Degree
	Peak I	Peak II	Peak III	
UL–TB	7.8/11.4	9.3/9.5	20.54/4.3	0.40
UL–TT	7.6/11.7	9.5/9.3	20.3/4.4	0.40
UL–MB	8.0/11.1	9.6/9.2	20.4/4.4	0.42
UL–MT	8.0/11.1	9.5/9.3	20.0/4.4	0.41

CONCLUSIONS

The castor-oil-based PUNL (UL) and PU films with different hard-segment compositions, such as MDI, TDI and TMP, and BDO, were successfully prepared. The MDI-based UL films exhibited higher σ_b's than TDI-based UL films because MDI favored the formation of hydrogen bonds, especially in the ordered domain. The UL films with TMP had higher σ_b's than UL films with BDO, which was attributed to the formation of a three-dimensional network from TMP. However, TMP hindered the hydrogen-bond formation in the hard segments caused by the highly steric hindrance. Thus, UL–MT films, which consisted of MDI-based PU prepolymer, NL, and TMP, had the highest σ_b's because of the relatively strong interaction between hard–hard and hard–soft

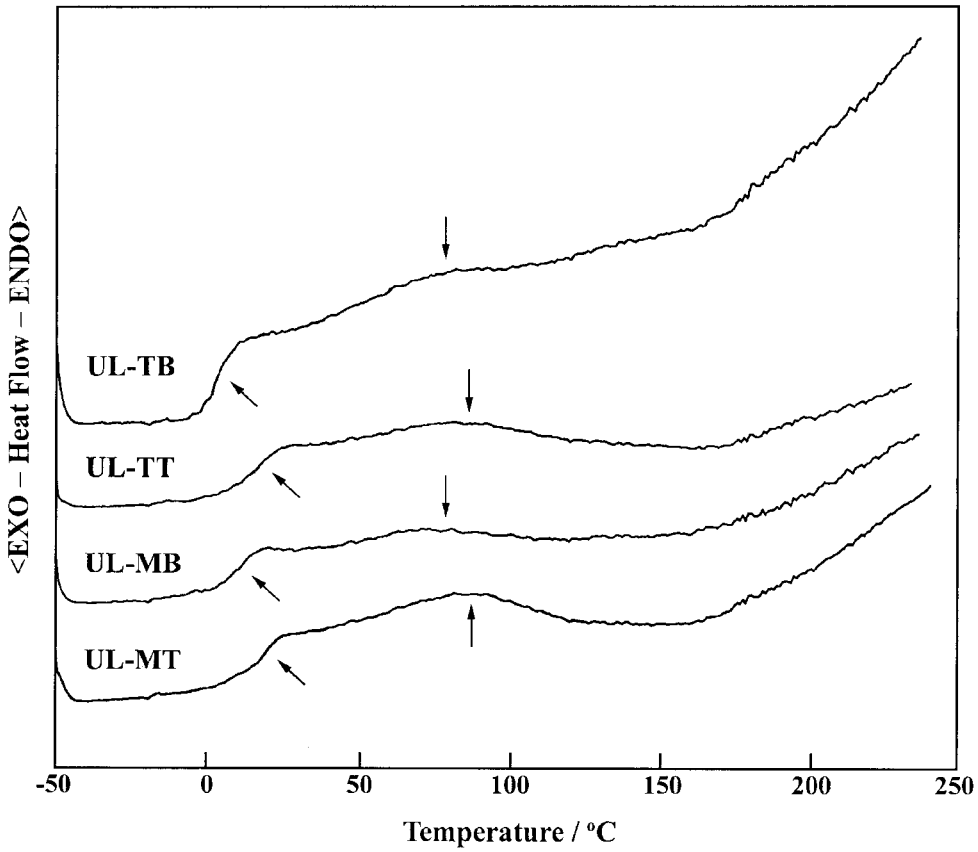

Figure 4 DSC curves as a function of temperature for the UL films.

segments imparted by MDI. Simultaneously, the MDI-based PU and UL films had lower *Re*'s than TDI-based films because of the flexibility imparted by —CH_2— groups in MDI. The values of σ_b and ϵ_b for the UL films with NL were much higher than those of the PU films, but the PU films were more fully and speedily resiled than the UL films, which suggests that the introduction of NL increased the interaction between hard segments by crosslinking and chain stiffness but decreased *Re*. The MDI-based UL films exhibited higher thermal stability than TDI-based UL films, whereas the other composites, such as TMP and BDO, hardly influenced the thermal stability. However, the UL–TB film, which contained TDL, NL, and BDO, had better flexibility at 0°C than others because of the microphase separation between soft and hard segments. The UL films with TMP exhibited higher T_{m2}'s than UL films with BDO with the same DI, which indicates that MDI

Table V Data of the UL Films Determined by DSC and DMA

Measure	UL–TB	UL–TT	UL–MB	UL–MT
T_{g1} (onset) (°C)	−0.34	9.77	3.49	11.60
$\Delta C_{p,g}$ ($\times 10^2$ J g^{-1} K^{-1})	59.51	34.97	42.41	37.52
T_{m2} (onset)/°C	55.25	56.92	45.6	52.65
ΔH_{m2} (J g)	6.90	6.61	4.27	12.01
T_g (onset) (°C)[a]	7.8	15.6	12.2	11.3
T_{max} (°C)[b]	19.4	35.0	25.3	33.4
Height of loss peak[b]	0.285	0.670	0.404	0.520

[a] Obtained from log E' versus T curves.
[b] Obtained from tan δ versus T curves.

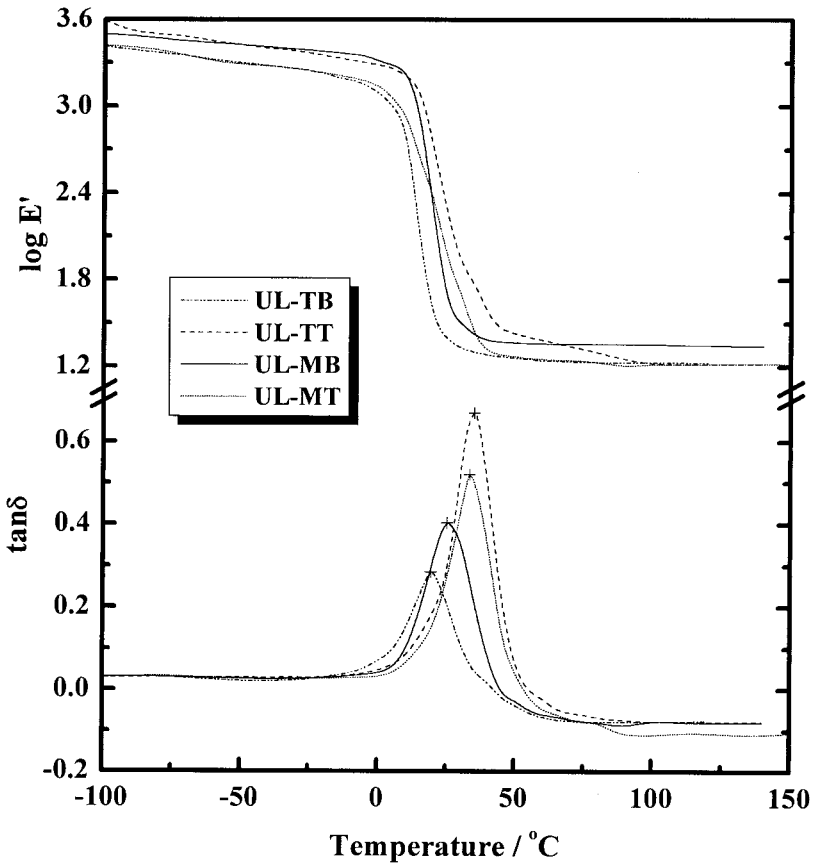

Figure 5 Storage modulus (E') and tan δ as a function of temperature for the UL films.

promoted the number of ordered hard-segment domains.

REFERENCES

1. Yu, L. T.; Lin, T. L.; Tsai, Y. M.; Liu, W. J. J Polym Sci Part B: Polym Phys 1999, 37, 2673.
2. Kim, H. D.; Lee, T. J.; Huh, J. H.; Lee, D. J. J Appl Polym Sci 1999, 73, 345.
3. Skarja, G. A.; Woodhouse, K. A. J Appl Polym Sci 2000, 75, 1522.
4. Luo, M.; Wang, D. N.; Ying, S. K. Polymer 1996, 37, 3045.
5. Lee, H. S.; Wang, Y. K.; Macknight, W. J.; Hsu, S. L. Macromolecules 1988, 21, 270.
6. West, J. C.; Cooper, S. L. J Polym Sci Polym Symp 1977, 60, 127.
7. Paik Sung, C. S.; Schneider, N. S. Macromolecules 1975, 8, 68.
8. Son, T. W.; Lee, D. W.; Lim, S. K. Polym J 1999, 31, 563.
9. Lin, T. L.; Yu, T. L.; Liu, W. J.; Tsai, Y. M. Polym J 1999, 31, 120.
10. Martin, D. J.; Meijs, G. F.; Renwick, G. M.; Gunatillake, P. A.; McCarthy, S. J. J Appl Polym Sci 1996, 60, 557.
11. Brunette, C. M.; Hsu, S. L.; Rossman, M.; Macknight, W. J.; Schneider, N. S. Polym Eng Sci 1981, 21, 668.
12. Paik Sung, C. S.; Hu, C. B.; Wu, C. S. Macromolecules 1980, 13, 111.
13. Schneider, N. S.; Paik Sung, C. S.; Matton, R. W.; Illinger, J. L. Macromolecules 1975, 8, 62.
14. Bras, W.; Derbyshire, G. E.; Greaves, G. N.; Mant, G. R.; Naylor, S.; Ryan, A. J. Mater Res Soc Symp Proc 1993, 302, 333.
15. Seefried, C. G.; Koleske, J. V.; Critchfield, F. E. J Appl Polym Sci 1975, 19, 2493.
16. Pandya, M. V.; Deshpande, D. D.; Hundiwale, D. G. J Appl Polym Sci 1986, 32, 4959.
17. Desai, S.; Thakore, I. M.; Sarawade, B. D.; Devi, S. Eur Polym J 2000, 36, 711.
18. Zhang, L.; Huang, J. J Appl Polym Sci 2001, 80, 1213.
19. Darren, J. M.; Gordon, F. M.; Gordon, M. R.; Pathiraja, A.; Gunatillake; Simon, J. M. J Appl Polym Sci 1996, 60, 557.